RSC Advances

ROYAL SOCIETY OF CHEMISTRY

www.rsc.org/advances

RSC Advances

PAPER

Solution-processable Low-bandgap 3-Fluorothieno[3,4-b]thiophene-2-carboxylate-based Conjugated Polymers for Electrochromic Applications

Received 00th January 20xx,
Accepted 00th January 20xx

DOI: 10.1039/x0xx00000x

www.rsc.org/

Zugui Shi,[a] Wei Teng Neo,[a,b] Ting Ting Lin,[a] Hui Zhou[a] and Jianwei Xu[a,c*]

In this paper, a series of low-bandgap donor-acceptor (D–A) conjugated polymers with 3-fluorothieno[3,4-b]thiophene-2-carboxylate (**FTT**) as an acceptor and ethylenedioxythiophene (**EDOT**) (**P1**), acyclic dioxythiophene (**AcDOT**) (**P2**) or propylenedioxythiophene (**ProDOT**) (**P3**) as donors were synthesized *via* Stille polymerization. The resultant polymers have good solubility in organic solvents. The polymers were characterized by gel permeation chromatography (GPC), nuclear magnetic resonance spectroscopy (NMR) and thermogravimetric analysis (TGA). Their electrochemical, morphological and electrochromic (EC) properties were investigated, and their absorption-transmission type electrochromic devices (ECDs) were fabricated and characterized. In their neutral states, the polymers displayed deep magenta (**P1**) to blue (**P2**, **P3**) hues, and upon electrochemical oxidation, they revealed grey tones with good optical contrasts (19-37 and 57-58% in visible and near-infrared (NIR) regions, respectively), good coloration efficiencies (158-380 and 279-378 cm^2/C for visible and NIR regions, resepctively) and reasonable redox stability (retaining 64-80% original optical contrast after 1000 cycles) under ambient conditions and without any encapsulation of the ECDs.

Introduction

Since electrochromism was first discovered by S. K. Deb and J. A. Chopoorian in 1966,[1] its intriguing optical properties have drawn tremendous interest from both the academic and industrial communities.[2-6] Successful application of electrochromic (EC) materials in anti-glazing vehicle rear mirrors, as well as smart windows for green buildings and high-end products, such as Boeing 787 dreamliner,[7,8] further triggered intensive attention to this field. Motivated by their great commercialization potentials, continuous research and development activities on EC materials ranged from inorganic metal oxides to organic small molecules and polymers. Among them, inorganic EC materials like Prussian blue, WO_3 and NiO were extensively studied and showed superior stability; however, the high expenditure of device fabrication, long switching time and limited color availability hampered their large-scale manufacturing as well as applications.[9-11] In contrast, the ease of solution-processability, fast switching rate and varieties of colors offered by organic EC materials have enabled them to be the next promising candidates.[12-15] Apart from well-documented viologen derivatives[16-21] and triphenylamine (TPA)-based polymers,[22-25] D–A alternating polymers are highly attractive owing to their intrinsic features such as band-gap fine tunability and enriched colors variation.[26-29] The majority of them are synthesized with the utilization of either benzotriazole[30,31] or benzothiadiazole as the electron-accepting unit.[32-40] In order to explore more potential acceptors for high performance D–A type EC polymers, our group has dedicated itself to the designing of new electron-deficient building blocks,[41, 42] as well as further investigations on reported acceptors which are previously used in other organic electronic applications such as organic photovoltaics or thin-film transistors.[43-45]

Fluorine is recognized as the smallest electron-withdrawing group with the highest Pauling electronegativity of 4.0, and it has been frequently used to fine tune the frontier molecular orbital energy levels of resulting organic materials.[46] Fluorinated organic materials have demonstrated unique chemical and physical properties, such as great thermal and chemical stability with elevated resistance towards degradation. These outstanding features have drawn intensive attention to investigate fluorinated molecules and their applications in organic photovoltaics (OPV),[47-53] organic field effect transistors (OFET)[54] as well as organic light-emitting diodes (OLED).[55] However, there are only a few examples of applying fluorinated compounds in organic electrochromic polymers. Recently, we demonstrated that introduction of fluorine atoms onto the polymer backbone had significant influence on the optical, electrochemical, and morphological

[a] *Institute of Materials Research and Engineering, Agency for Science, Technology and Research (A*STAR), 2 Fusionopolis Way, #08-03, Innovis, Singapore 138634; Email: jw-xu@imre.a-star.edu.sg*
[b] *NUS Graduate School for Integrative Science and Engineering, National University of Singapore, 28 Medical Drive, Singapore 117456.*
[c] *Department of Chemistry, National University of Singapore, 3 Science Drive 3, Singapore 117543.*
Electronic Supplementary Information (ESI) available: [details of any supplementary information available should be included here]. See DOI: 10.1039/x0xx00000x

properties of the polymers.[56] Encouraged by these findings, herein, we report a series of narrow-bandgap D–A polymers employing 3-fluorothieno[3,4-b]thiophene-2-carboxylate (FTT) as the electron-withdrawing acceptor,[57, 58] as well as their electrochromic properties.

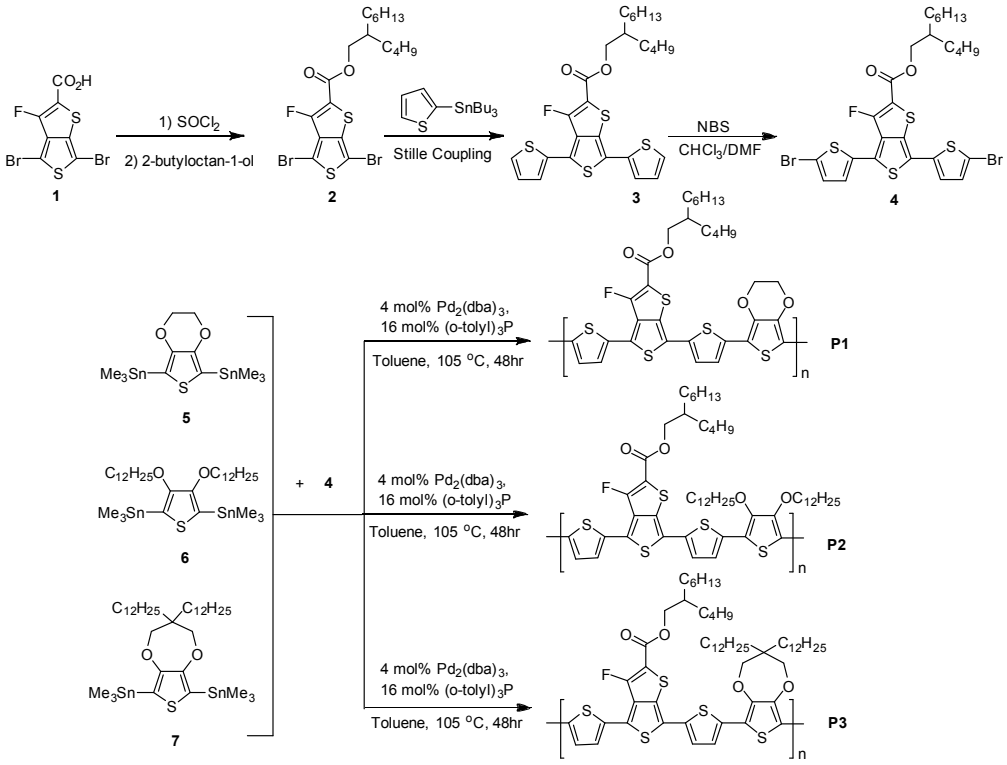

Scheme 1. Synthetic routes of monomers and polymers **P1-P3**.

Results and Discussion

Synthesis and characterization of polymers

The synthesis leading to polymers **P1-P3** is shown in Scheme 1. First, 4,6-dibromo-3-fluorothieno[3,4-b]thiophene-2-carboxylic acid (**1**) was converted to 2-butyloctyl 4,6-dibromo-3-fluorothieno[3,4-b]thiophene-2-carboxylate (**2**) in a one-pot esterification reaction with 76% yield. Subsequent microwave-assisted Stille coupling of **2** with tributylthiophenestanne, followed up by bromination, gave monomer **4**. Monomers **5**, **6** and **7** were synthesized according to reported procedures in literatures.[36,59] Finally, **P1-P3** were obtained by reacting monomer **4** with **5**, **6** and **7** in the presence of palladium

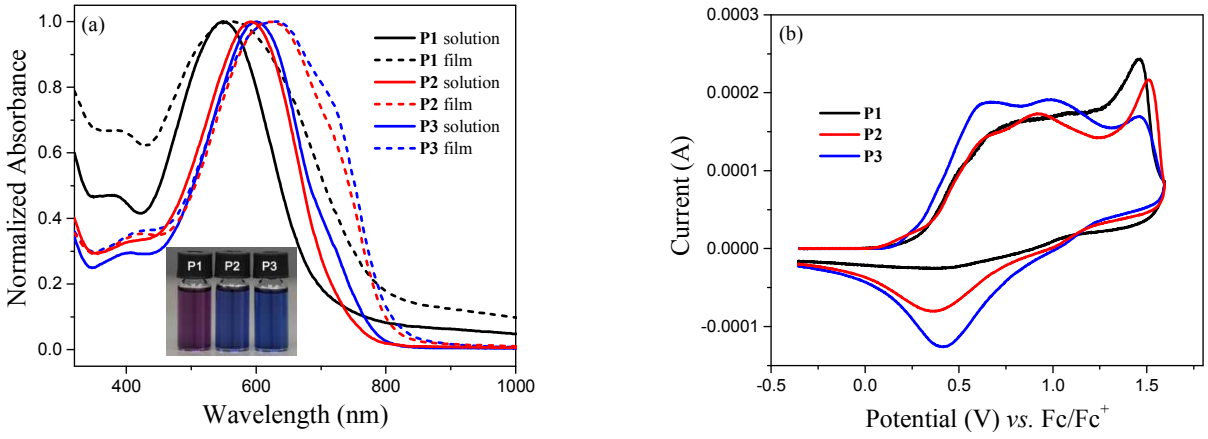

Figure 1. (a) Normalized UV-vis absorption spectra of **P1-P3** in chlorobenzene and as thin films. Insert:Photos of **P1-P3** dilute solutions in chlorobenzene. (b) Cyclic voltammograms of **P1-P3** thin films.

ARTICLE

catalyst $Pd_2(dba)_3$ with 57-71% yields. Both polymers **P2** and **P3** displayed much better solubility than **P1** in common organic solvents such as hexane due to the presence of more alkyl chains. All polymers exhibited good thermal stability with decomposition temperatures of more than 300 °C (Table 1).

Table 1. Synthetic yields, molecular weights, polydispersity and thermal data of polymers.

Polymer	Yield (%)	M_n (kDa)[a]	M_w (kDa)[b]	PDI	Td (in N_2) (°C)[c]
P1	57	1.8	2.9	1.6	307
P2	68	7.3	14.6	2.0	335
P3	71	5.5	8.3	1.5	366

[a] Number average molecular weight; [b] Weight-average molecular weight; [c] Decomposition temperature at which 5 % weight loss occurs.

Optical properties

The UV-vis absorption spectra of **P1**-**P3** in both solution and thin film states are shown in Figure 1a. All three polymers reveal asymmetric dual absorption bands with the lower-intensity and higher-intensity peaks centered at approximately 400 and 600 nm respectively. While the spectra for both **P2** and **P3** are largely similar, **P1** exhibits significant blue-shifted absorptions maximum and onsets. Going from the solution to film states, considerable spectra broadening in addition to bathochromic shifts and the formation of vibronic shoulders suggest the strong π-π stacking and aggregation of the polymers in the solid state. Estimation of the optical band gaps of the polymers was obtained from the absorption onset in thin films, which generally decrease across **P1**-**P3**, from 1.62 to 1.55 to 1.54 eV respectively.

Electrochemical properties

Cyclic voltammetry was employed to investigate the redox behaviour of the polymers. The cyclic voltammograms of the polymer thin films are shown in Figure 1b. Polymers **P1-P3** revealed two quasi-reversible redox processes, with similar oxidation onsets of approximately 0.2 V *vs* the ferrocene/ferrocenium redox couple. Based on the oxidation onsets, the highest occupied molecular orbital (HOMO) levels of **P1**-**P3** were estimated to be from -4.87 to -4.96 eV. Due to the lack of a distinct n-doped reduction peak, the lowest unoccupied molecular orbital (LUMO) levels of the polymers were estimated from the optical band gaps. Both oxidation and reduction potentials of **P2** and **P3** are decreased in comparison with that of **P1** due to the attachment of two electron-donating alkoxy groups in one thiophene unit in **P2** and **P3**. A summary of the optical and electrochemical properties is provided in table 2.

Table 2. Summary of optical and electrochemical properties of polymers.

	λmax (nm)		λonset (nm)		Egopt (eV)[a]	E_{onset} (V)[b]	E_{ox} (V)[b]	E_{red} (V)[b]	HOMO (eV)[c]	LUMO (eV)[d]
	Solution	Film	Solution	Film						
P1	549	562	691	765	1.62	0.16	0.70, 1.09	0.44	-4.96	-3.34
P2	591	620	743	798	1.55	0.07	0.63, 0.91	0.36	-4.87	-3.32
P3	600	627	778	804	1.54	0.15	0.65, 0.98	0.42	-4.95	-3.41

[a] $E_g^{opt} = 1240/\lambda_{onset,film}$; [b] Values reported vs ferrocene; [c] $E_{HOMO} = -(E_{onset,ox\ vs\ ferrocene})-4.8$; [d] $E_{LUMO} = E_{HOMO} + E_g^{opt}$.

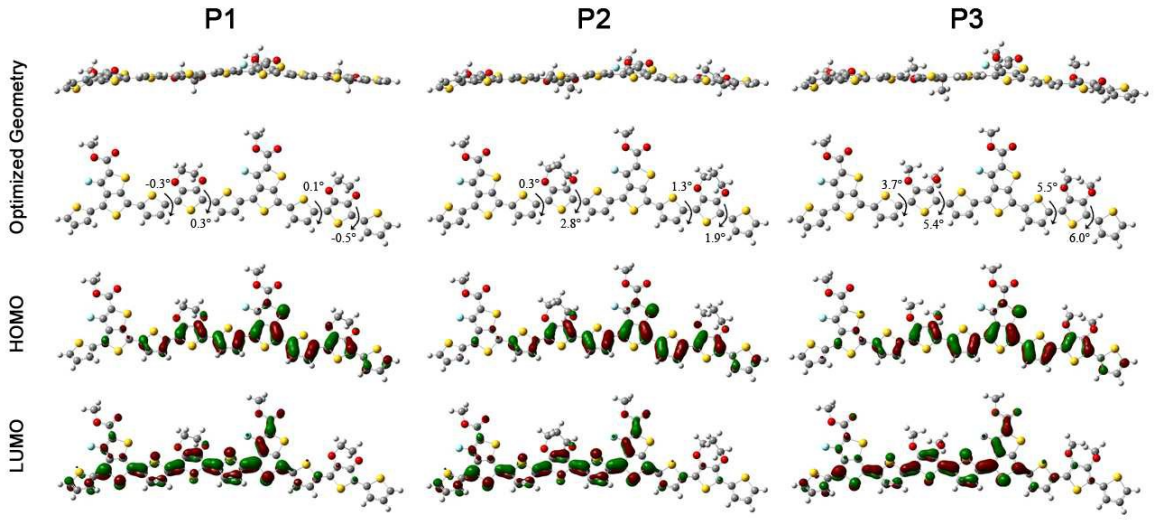

Figure 2. Optimized geometries and charge-density isosurfaces for the HOMO and LUMO levels of **P1**-**P3** dimers (B3LYP/6-31G).

ARTICLE

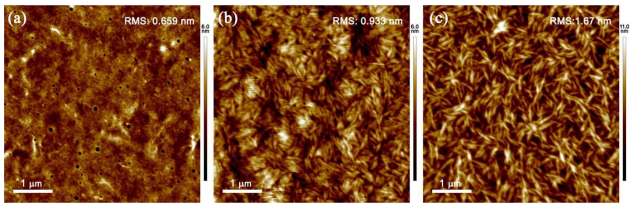

Figure 3. AFM images of spin-coated (a**) P1**, (b) **P2** and (c) **P3** thin films. Image size: 5×5 µm.

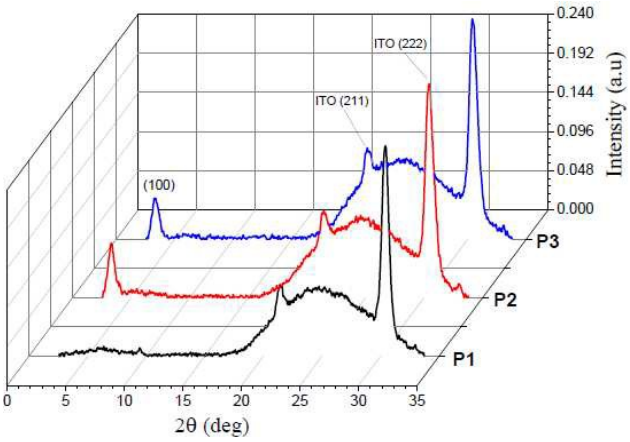

Figure 4. XRD plots of **P1**-**P3** thin films dropcast on ITO/glass substrates.

Computational calculations

The minimum-energy conformations of **P1**-**P3** were probed using time-dependent density functional theory (TD-DFT) calculations at B3LYP/6-31G(d) theory level for the dimeric model compounds. For simplification, all alkoxy and alkyl side chains are replaced with methoxy and methyl groups respectively. To evaluate the extent of effective conjugation in the polymers, the dihedral angles between EDOT, ProDOT as well as AcDOT with the adjacent thiophene rings were analysed (Figure 2). Going from **P1** to **P3**, the dihedral angles increase from -0.5 – 0.3°, 0.3 – 2.8° to 3.7 – 6.0°. This suggests that molecular planarity and conjugation of π-orbitals is the highest for **P1**, followed by **P2** and subsequently **P3**, and hence, the absorptions should be blue-shifted systematically from **P1** to **P3**. Surprisingly, observed optical and electrochemical properties reflect the opposite trend. One plausible reason is that the long alkyl and alkoxy side chains of ProDOT and AcDOT in **P2** and **P3** respectively enhances the van der Waals interactions with the side chains on the acceptor unit, which aids the packing of the polymer chains.

Thin film morphology

AFM was employed for the analysis of surface morphologies of the polymer thin films. The height images are shown in Figure 3. The results reveal striking differences in the packing and alignment of the polymer chains. For **P1**, a relatively smooth and homogeneous surface was observed without any obvious and defined structures. On the other hand, both **P2** and **P3** exhibit distinct fibrillar crystalline domains. While the individual polymer fibres appear to be shorter and pack more closely in **P2**, the fibrillar structures are longer and seem to be more spaced out in **P3**, thus giving rise to a more open and porous morphology.

The increased alignment and packing of the polymer chains in **P2** and **P3** thin films as observed from the optical and AFM studies is verified from XRD measurements (Figure 4). At around 3°, a sharp and definite diffraction (100) peak that corresponds to in-plane spacing is observed for both **P2** and **P3**, which is absent for **P1**.

Electrochromic properties

Color and spectral changes of **P1**-**P3** under various applied potentials were probed *in-situ*, on fabricated absorption/ transmission type ECDs. The spectroelectrochemical graphs and hues of the ECDs are shown in Figure 5. In their neutral states, both **P2** and **P3** reveal almost identical colors, with minimal difference in the intensity of blue tones (b* values: -27 for **P2** and -29 for **P3**). In contrast, **P1** display a dark magenta hue, owing to the strong absorption of red tones (positive a* value) unlike the other polymers. As the ECDs are progressively oxidized from the neutral states, the absorptions in the visible region for all three polymers deplete while strong and broad NIR absorption bands are gradually formed as a result of the generation of polarons and bipolarons. The observed NIR peak at approximately 900 nm, attributed to the formation of polarons, reaches a maximum in intensity at around 1.8 V. Above that potential, further generation of polarons is suppressed and instead, the polarons appear to be converted to the bipolarons as seen from the extended increase in absorptions near 1200 nm. For both **P2** and **P3**, the polymers are fully oxidized at 2.0 V as observed from the complete depletion of the initial absorptions in the visible region, albeit the occurrence of slight tailing into the 600-750 nm range. On the other hand, residual absorption is still much present in **P1**. This could be due to its lowered susceptibility towards oxidation as a result of limitation in charge hopping owing to reduced polymer packing and crystallinity. Hence, **P1** exhibits a darker grey tone at 2.0 V. For **P2** and **P3**, better device transmissivities are observed, with L* values of 82 and 80 respectively in comparison to **P1** with 73. For the characterization of electrochromic performance such as optical contrasts, switching times and coloration efficiencies, a square-wave potential step absorptiometry was utilized. Redox potentials at +1.6 and -1.6 V were employed. The transmittance changes of the ECDs as a function of time were recorded in both the visible and NIR regions. Figure 6 illustrates the switching cycles of **P1**-**P3** ECDs and a summary of the device properties is given in Table 3. Both **P2** and **P3** reveal very similar contrasts (around 37 and 58 % in the visible

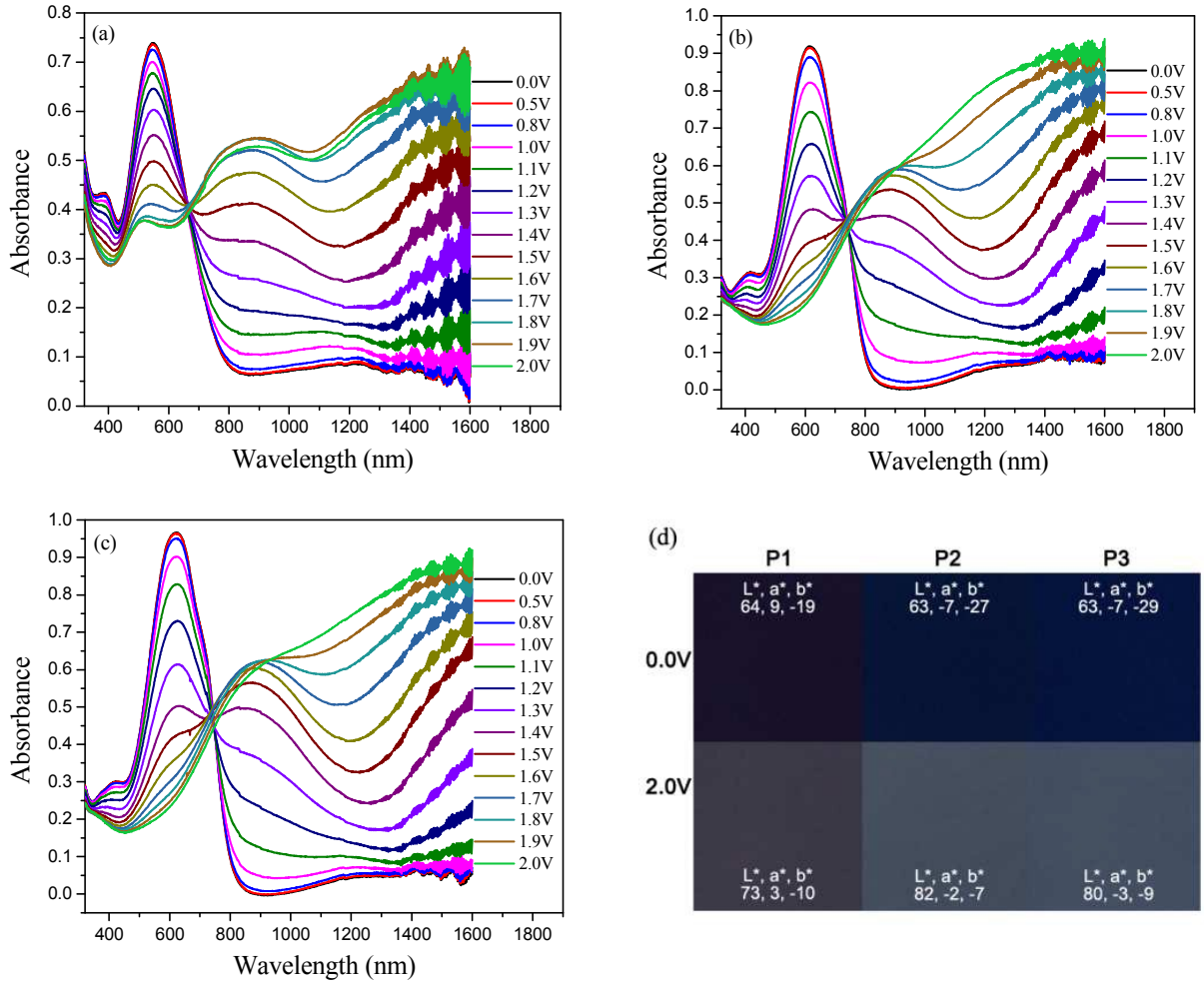

Figure 5. Spectroelectrochemical graphs of (a) **P1**, (b) **P2** and (c) **P3** devices at various applied potentials. (d) L*, a*, b* color coordinates (following the Commission Internationale de l'Eclairage 1976 *L*a*b** color model) of **P1-P3** devices in their neutral and oxidized states.

and NIR regions respectively) and switching kinetics. On the contrary, device performance for **P1** is poorer with lower with lower contrasts and slower switching speeds. This finding suggests that besides the chemical makeup and chain-packing characteristic, the molecular weight of the polymers may be a critical factor affecting the electrochromic performance. Polymers with higher molecular weights tend to yield high performance in most organic electronics, especially in solar cells and thin-film transistors.[60,61] Therefore, it may be worthwhile to probe deeper into the effect of molecular weight of polymers on their electrochromic properties. Across all polymers, the asymmetry in bleaching and coloration times can be ascribed to the difference in conductivity of the polymer films between the neutral and oxidized states-semiconducting in their neutral states and conducting in their oxidized states.[62] It is also observed that **P1** shows an inferior coloration efficiency compared to **P2** and **P3**. This could most likely be related to the film morphologies as described in the earlier section. Unlike **P2** and **P3** with higher polymer chain alignment and crystallinity, the film morphology of **P1** is much more compact and denser as the polymer aggregates in a random fashion. The lack of openness and porosity in **P1** film hinders the penetration of counter ions during the redox reaction, in addition to the lack of provision of accessible sites for electrochemical reactions. While several insights have been revealed for the kind of morphological structure optimal for electrochromic devices, deliberate methods to obtain such desired morphologies are still lacking. The long-term stability testing for **P1**-**P3** ECDs was carried out by monitoring the optical contrast over repeated redox cycles, between +1.6 and -1.6 V and at a switching time of 20 s. An equilibrium period of about 60 cycles was allowed for all the devices. The switching cycles for **P2** ECD are depicted in Figure 7, as an example. Over 1000 deep potential steps, polymer **P2** retained 80 % of its initial contrast, suggesting good ambient redox stability despite the lack of additional encapsulation. For **P1** and **P3**,

ARTICLE

Table 3. Summary of Electrochromic Performance of ECDs.

Polymer	Thickness (nm)	Visible (λ_{max})[a]				NIR (1500 nm)			
		Contrast (%)	τ_b (s)[b]	τ_c (s)[c]	CE (cm^2/C)[d]	Contrast (%)	τ_b (s)[b]	τ_c (s)[c]	CE (cm^2/C)[d]
P1	140	19.2	61.9	5.47	158	56.5	17.7	30.7	279
P2	160	36.9	43.1	2.41	325	58.3	3.15	28.2	344
P3	175	37.3	42.9	2.17	380	57.2	2.06	33.2	378

[a] 548, 616 and 622 nm for **P1**, **P2** and **P3** respectively; [b] Bleaching time where bleaching refers to the process in which the percent transmittance changes from a lower value to a higher value; [c] Coloration time where coloration refers to the process in which the percent transmittance changes from a higher value to a lower value; [d] Coloration efficiency.

about 70 and 64 % of the optical contrasts were sustained over 1000 repeated cycles respectively.

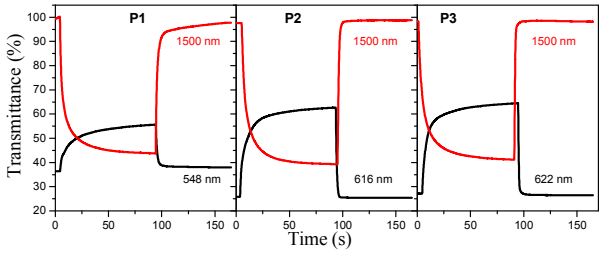

Figure 6. Switching cycles of **P1**-**P3** devices in the visible (λ_{max}) (black line) and NIR (1500 nm) (red line) regions between +1.6 and -1.6 V.

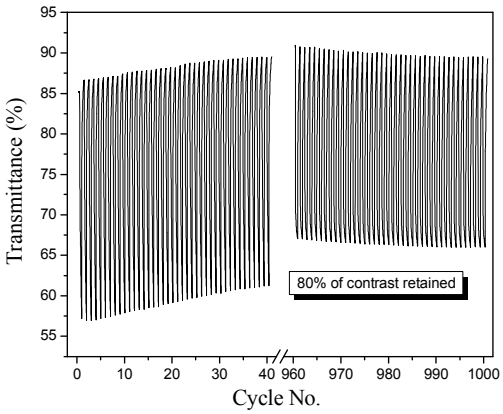

Figure 7. Stability testing and degradation profiles of **P2** devices monitored at 1500 nm.

Conclusion

A series of novel D-A conjugated polymers based on FTT as the acceptor were synthesized *via* Stille coupling. The polymers exhibited saturated magenta and blue neutral-state hues, with distinct colored-to-transmissive reversible electrochromic switching under applied potentials of +1.6 and -1.6 V. High optical contrasts of about 40 and 60 % were obtained in the visible and NIR regions respectively, with reasonable switching speeds of a few to tens of seconds as well as coloration efficiencies of up to 380 cm^2/C. Despite fabrication and testing under ambient conditions, the devices displayed promising redox stability by sustaining between 64 to 80 % of their initial optical contrasts over 1000 potential cycles. These properties would render such polymers to be potential candidates as electrochromic materials, and enhanced performance would be achieved upon further device optimization.

Experimental

Materials

4,6-dibromo-3-fluorothieno[3,4-b]thiophene-2-carboxylic acid was purchased from Sunatech Inc., and used as received. Other chemicals were purchased from Sigma-Aldrich, and used without further treatments. ITO-coated glass substrates (15 Ω/sq, 35×30×1.1mm) were purchased from Xinyan Technology Ltd.

2-butyloctyl 4, 6-dibromo-3-fluorothieno[3, 4-b]thiophene-2-carboxylate (2)

4,6-dibromo-3-fluorothieno[3,4-b]thiophene-2-carboxylic acid (2 mmol) was dispersed in 20 mL of thionyl chloride. The mixture was refluxed under nitrogen atmosphere overnight. After completion of reaction, excess thionyl chloride was removed and a yellow solid product obtained. The solid and 2-butyloctan-1-ol (4 mmol) were subsequently dissolved in anhydrous THF. Triethylamine (4 mmol) and dimethylaminopyridine (0.2 mmol) were then added at 0 °C under nitrogen atmosphere. The reaction mixture was stirred at room temperature for 12 h. After removal of the solvent, the residue was subjected to column chromatography with eluent (hexane:ethyl acetate= 10:1), giving an oil product in 76% yield. ^{1}H NMR (400 MHz, $CDCl_3$) δ (ppm) 4.22 (d, *J* = 5.2 Hz, 2H), 1.73 (d, *J* = 5.6 Hz, 1H), 1.37-1.29 (m, 16H), 0.90-0.86 (m, 6H).

2-butyloctyl 3-fluoro-4, 6-di(thiophen-2-yl)thieno[3, 4-b]thiophene-2-carboxylate (3)

To a solution of 2-butyloctyl 4, 6-dibromo-3-fluorothieno[3,4-b]thiophene-2-carboxylate (**2**) (1.5 mmol) and tributyl(thiophen-2-yl)stannane (4.5 mmol) in degassed

DMF/toluene (5 mL + 5 mL) was added $PdCl_2(PPh_3)_2$ (0.07 mmol). The reaction mixture was heated under 120 °C under microwave for 2 min, and then stirred at 160 °C for 20 min. The reaction mixture was extracted with dichloromethane, washed with brine, dried over $MgSO_4$ and filtered through Celite. The solvent was removed by evaporation and the residue was purified by chromatography to give the product in 90% yield as yellow oil. ^{1}H NMR (400MHz, $CDCl_3$) δ (ppm) 7.41 (s, 1H), 7.38-7.35 (m, 2H), 7.25 (d, *J* = 4.4 Hz, 1H), 7.12-7.09 (m, 2H), 4.24 (d, *J* = 5.6 Hz, 2H), 1.76 (d, *J* = 5.6 Hz, 1H), 1.42-1.29 (m, 16H), 0.92-0.86 (m, 6H).

2-butyloctyl 4, 6-bis(5-bromothiophen-2-yl)-3-fluorothieno[3, 4-b]thiophene-2-carboxylate (4)

To a solution of compound **3** (1.2 mmol) in 10 mL chloroform in an ice-water bath, N-bromosuccinimide (2.5 mmol) was slowly added. The reaction was completed within 1 h. Purification using column chromatography (hexane/EA=20:1) and recrystallization from ethanol gave a red solid product (95% yield). ^{1}H NMR (400MHz, $CDCl_3$) δ (ppm) 7.13 (d, *J* = 4.0 Hz, 1H), 7.06-7.05 (m, 2H), 6.98 (d, *J* = 4.0 Hz, 1H), 4.24 (d, *J* = 5.6 Hz, 2H), 1.76 (d, *J* = 5.6 Hz, 1H), 1.38-1.30 (m, 16H), 0.92-0.87 (m, 6H).

General procedure for Stille copolymerization.

Tris(dibenzylideneacetone)palladium (0.04 mmol) and tri(o-tolyl)phosphine (0.032 mmol) were added to a solution comprising of a mixture of 4 (0.2 mmol) and 5 (0.2 mmol) in anhydrous toluene (5 mL) in the glove box. The mixture was stirred at 105 °C for 48 h. Subsequently, the reaction mixture was precipitated into 100 mL methanol and 15 mL concentrated hydrochloric acid. After stirring overnight, the polymer was collected by suction filtration and subjected to Soxhlet extraction with methanol (12 h), ethyl acetate (12 h), hexane (12 h), and chloroform (12 h). The chloroform fraction was then concentrated, precipitated into 150 mL methanol, filtered and dried in a vacuum oven to obtain the final product **P1**. Polymers **P2** and **P3** were prepared using the same method.

Electrochromic device fabrication

ITO/glass substrates were cleaned by successive ultrasonication in acetone, isopropyl alcohol and distilled water, and blown dry with N_2 prior to use. Polymer solutions of **P1**-**P3** were prepared at a concentration of 15 mg/mL in 1:3 (v/v) chloroform:chlorobenzene. Polymer films were prepared by spin-coating the prepared solutions (350 rpm, 60 s) onto the ITO substrates. The polymer solutions were filtered prior to spin-coating. Excessive polymer edges were subsequently removed by swabbing with chloroform using a cotton bud to obtain an active area of 2 × 2 cm^2. On a second piece of ITO substrate, an area of 2 × 2 cm2 was blocked out using parafilm. The total thickness of the parafilm spacer and barrier was kept constant at 0.01". 250 µL of the gel electrolyte (0.512 g of lithium perchlorate and 2.8 g of poly(methyl methacrylate) (MW = 120 000 g/mol) in 6.65 ml of propylene carbonate and 28 ml of dry acetonitrile) was pipetted within the area and left to dry for 5 minutes. The electrochromic device (ECD) was fabricated by assembling the two ITO/glass substrates together with the polymer film and gel electrolyte in contact.

Instrumentation

^{1}H and ^{13}C NMR were performed using a Bruker Avance 400 spectrometer. TGA was performed using a TGA Q500 from TA Instruments. Gel permeation chromatography was carried out at room temperature using an Alliance Waters 2690 HPLC/GPC system, with HPLC grade THF as the eluent and PMMA as the standard. All UV-vis/UV-vis-NIR absorption spectra were recorded on a Shimadzu UV-3600 UV-vis-NIR spectrophotometer. Cyclic voltammetry experiments were carried out using an Autolab PGSTAT128N potentiostat. Measurements were done in a MBraun LABmaster 130 glove box, in a three-electrode cell configuration with polymer-coated glassy carbon, Pt wire and Ag wire as the working, counter and pseudo-reference electrodes respectively. A 0.1 M $LiClO_4$/ACN electrolyte/solvent couple was used and all measurements were recorded at 50 mV/s. The pseudo-reference electrode was calibrated against the ferrocene/ferrocenium redox couple. All electrochromic studies were performed *in-situ*, using both the potentiostat and spectrophotometer. AFM images were obtained under tapping mode, using a Bruker Dimension Icon™ atomic force microscope. X-ray diffraction (XRD) patterns of the thin films were recorded in reflection mode with a Cu-Kα radiation source (λ = 0.15406 nm) on a Bruker D8 General Area Detector Diffraction System. Thicknesses of the polymer films were measured using a KLA Tencor P16 surface profiler. CIE L*, a*, b* values of the devices were reported under outdoor daylight illumination (65/10°) and measured using a Hunterlab ColorQuest XE.

Acknowledgements

This study was supported by the Agency for Science, Technology and Research (A* STAR) and Ministry of National Development (MND) Green Building Joint Grant (No. 1321760011), Singapore. This work was also supported by the A*STAR Computational Resource Centre through the use of its high performance computing facilities. We would like to thank Mr. Lim Poh Chong for the XRD images.

Notes and references

1 S. K. Deb and J. A. Chopoorian, *J. Appl. Phys.*, 1966, **37**, 4818.
2 T. Yamase, *Chem. Rev.*, 1998, **98**, 307.
3 C. G. Granqvist, A. Azens, A. Hjelm, L. Kullman, G. A. Niklasson, D. Rönnow, M. S. Mattsson, M. Veszelei and G. Vaivars, *Sol. Energy,* 1998, **63**, 199.
4 US Pat., US7874666B2, 2011.
5 P. A. Ersman, J. Kawahara and M. Berggren, *Org. Electron.,* 2013, **14**, 3371.
6 P. Andersson, R. Forchheimer, P. Tehrani and M. Berggren, *Adv. Funct. Mater.,* 2007, **17**, 3074.

7 J. Jacob, H. Markus, L. D. Aubrey and C. K. Frederik, *Adv. Funct. Mater.*, 2015, **25**, 2073.
8 C. G. Granqvist, *Thin Solid Films*, 2014, **564**, 1.
9 S. H. Lee, R. Deshpande, P. A. Parilla, K. M. Jones, B. To, A. H. Mahan and A. C. Dillon, *Adv. Mater.*, 2006, **18**, 763.
10 L. Liu, M. Layani, S. Yellinek, A. Kamyshny, H. Ling, P. S. Lee, S. Magdassi and D. Mandler, *J. Mater. Chem. A*, 2014, **2**, 16224.
11 C.-P. Li, C. A. Wolden, A. C. Dillon and R. C. Tenent, *Sol. Energ. Mat. Sol. Cells*, 2012, **99**, 50.
12 P. Shi, C. M. Amb, A. L. Dyer and J. R. Reynolds, *ACS Appl. Mater. Interfaces,* 2012, **4**, 6512.
13 B. D. Reeves, C. R. G. Grenier, A. A. Argun, A. Cirpan, T. D. McCarley and J. R. Reynolds, *Macromolecules*, 2004, **37**, 7559.
14 P. Chandrasekhar, B. J. Zay, C. Cai, Y. Chai and D. Lawrence, *J. Appl. Polym.Sci.,* 2014, **131**, 41043.
15 H. W. Heuer, R. Wehrmann and S. Kirchmeyer, *Adv. Funct. Mater*., 2002, **12**, 89.
16 K. Bange and T. Gambke, *Adv. Mater*., **1990**, *2*, 10.
17 H. C. Ko, S. Kim, H. Lee and B. Moon, *Adv. Funct. Mater*., **2005**, *15*, 905.
18 K. Murugavel, *Polym. Chem*., **2014**, *5*, 5873.
19 N. Jordão, H. Cruz, A. Branco, C. Pinheiro, F. Pina and L. C. Branco, *RSC Adv*., 2015, **5**, 27867.
20 R. Nakajima, Y. Yamada, T. Komatsu, K. Murashiro, T. Saji and K. Hoshino, *RSC Adv*., 2012, **2**, 4377.
21 L. Wang, L. Yuan, X. Wu, J. Wu, C. Hou and S. Feng, *RSC Adv*., 2014, **4**, 47670.
22 H. Jin, J. Tian, S. Wang, T. Tan, Y. Xiao and X. Li, *RSC Adv*., 2014, **4**, 16839.
23 J. Lin, X. Ni, *RSC Adv*., 2015, **5**, 14879.
24 T. Abidin, Q. Zhang, K.-L. Wang and D.-J. Liaw, *Polymer*, 2014, **55**, 5293.
25 H.-J. Yen and G.-S. Liou, *Polym. Chem.*, 2012, **3**, 255.
26 G. Gunbas and L. Toppare, *Chem. Commun.,* 2012, **48**, 1083.
27 H. Akpinar, A. Balan, D. Baran, E. K. Ünver and L. Toppare, *Polymer*, 2010, **51**, 6123.
28 C. M. Cho, Q. Ye, W. T. Neo, T. Lin, X. Lu and J. Xu, *Polym. Chem.*, 2015, **5**, 7570.
29 G. Ding, C. M. Cho, C. Chen, D. Zhou, X. Wang, A. Y. X. Tan, J. Xu and X. Lu, *Org. Electron.,* 2013, **14**, 2748.
30 A. Balan, D. Baran and L. Toppare, *Polym. Chem.*, 2011, **2**, 1029.
31 G. Hzalan, A. Balan, D. Baran and L. Toppare, *J. Mater. Chem.*, 2011, **21**, 1804.
32 A. Balan, G. Gunbas, A. Durmus and L. Toppare, *Chem. Mater.*, 2008, **20**, 7510.
33 P. Shi, C. M. Amb, E. P. Knott, E. J. Thompson, D. Y. Liu, J. Mei, A. L. Dyer and J. R. Reynolds, *Adv. Mater*., 2010, **22**, 4949.
34 P. M. Beaujuge and J. R. Reynolds, *Chem. Rev*., 2010, **110**, 268.
35 P. M. Beaujuge, S. Ellinger and J. R. Reynolds, *Adv. Mater*., 2008, **20**, 2772.
36 P. M. Beaujuge, S. V. Vasilyeva, D. Y. Liu, S. Ellinger, T. D. McCarley and J. R. Reynolds, *Chem. Mater.,* 2012, **24**, 255.
37 P. M. Beaujuge, S. Ellinger and J. R. Reynolds, *Nat. Mater*., 2008,**7**, 795.
38 P. M. Beaujuge, C. M. Amb and J. R. Reynolds, *Acc. Chem. Res.*, 2010, **43**, 1396.
39 M. Karakus, A. Balan, D. Baran, L. Toppare and A. Cirpan, *Synt. Met.*, 2012, **162**, 79.
40 M. Sendur, A. Balan, D. Baran, B. Karabay and L. Toppare, *Org. Electron.*, 2010, **11**, 1877.
41 Q. Ye, W. T. Neo, C. M. Cho, S. W. Yang, T. Lin, H. Zhou, H. Yan, X. Lu, C. Chi and J. Xu, *Org. Lett.*, 2014, **16**, 6386.
42 Q. Ye, W. T. Neo, T. Lin, J. Song, H. Yan, H. Zhou, K. W. Shah, S. J. Chua and J. Xu, *Polym. Chem.*, 2015, **6**, 1487.
43 W. T. Neo, L. M. Loo, J. Song, X. Wang, C. M. Cho, H. S. On Chan, Y. Zong and J. Xu, *Polym. Chem*., 2013, **4**, 4663.
44 W. T. Neo, Z. Shi, C. M. Cho, S.-J. Chua and J. Xu, *ChemPlusChem*, 2015, **80**, 1298.
45 J. Z. Low, W. T. Neo, Q. Ye, W. J. Ong, I. H. K. Wong, T. T. Lin and J. Xu, *J. Polym. Sci. A Polym. Chem.*, 2015, **53**, 1287.
46 F. Babudri, G. M. Farinola, F. Naso and R. Raqni, *Chem. Commun.*, 2007, 1003.
47 H. Zhou, L. Yang, A. C. Stuart, S. C. Price, S. Liu and W. You, *Angew. Chem. Int. Ed*., 2011, **50**, 2995.
48 Z. Li, J. Lu, S.-C. Tse, J. Zhou, X. Du, Y. Tao and J. Ding, *J. Mater. Chem*., 2011, **21**, 3226.
49 G. Li, C. Kang, X. Gong, J. Zhang, W. Li, C. Li, H. Dong, W. Hu and Z. Bo, *J. Mater. Chem*. C, 2014, **2**, 5116.
50 Z. Chen, P. Cai, J. Chen, X. Liu, L. Zhang, L. Lan, J. Peng, Y. Ma and Y. Cao, *Adv. Mater*., 2014, **26**, 2586.
51 N. Wang, Z. Chen, W. Wei and Z. Jiang, *J. Am. Chem. Soc*., 2013, **135**, 17060.
52 J.-F. Jheng, Y.-Y. Lai, J.-S. Wu, Y.-H. Chao, C.-L. Wang and C.-S. Hsu, *Adv. Mater*., 2013, **25**, 2445.
53 Y. Wang, X. Xin, Y. Lu, T. Xiao, X. Xu, N. Zhao, X. Hu, B. S. Ong and S. C. Ng, *Macromolecules,* 2013, **46**, 9587.
54 T. Lei, J.-H. Dou, Z.-J. Ma, C.-H. Yao, C.-J. Liu, J.-Y. Wang and J. Pei, *J. Am. Chem. Soc*., 2012, **134**, 20025.
55 U. Giovanella, C. Botta, F. Galeotti, B. Vercelli, S. Battiato and M. Pasini, *J. Mater. Chem. C*, 2013, **1**, 5322.
56 W. T. Neo, K. H. Ong, T. T. Lin, S.-J. Chua and J. Xu, *J. Mater. Chem. C*, 2015, **3**, 5589.
57 Y. Liang, D. Feng, Y. Wu, S.-T. Tsai, G. Li, C. Ray and L. Yu, *J. Am. Chem. Soc.*, 2009, **131**, 7792.
58 Y. Liang, Z. Xu, J. Xia, S.-T. Tsai, Y. Wu, G. Li, C. Ray and L. Yu, *Adv. Mater.*, 2010, **22**, E135.
59 M. Turbiez, P. Frère, M. Allain, C. Videlot, J. Ackermann and J. Roncali, *Chem. Eur. J.*, 2005, **11**, 3742.
60 J. Li, Y. Zhao, H. S. Tan, Y. Guo, C.-A. Di, G. Yu, Y. Liu, M. Lin, S. H. Lim, Y. Zhou, H. Su and B. S. Ong, *Sci. Rep.,* 2012, **2**, 754.
61 T.-Y. Chu, J. Lu, S. Beaupré, Y. Zhang, J.-R. Pouliot, J. Zhou, Am Najari, M. Leclerc and Y. Tao, *Adv. Funct. Mater.,* 2012, **22**, 2345.
62 T. Johansson, L. A. A. Pettersson, O. Inganäs, *Synt. Met.*, 2002, **129**, 269.

Solution-processable Low-bandgap 3-Fluorothieno[3,4-b]thiophene-2-carboxylate-based Conjugated Polymers for Electrochromic Applications

Zugui Shi,[a] Wei Teng Neo,[a,b] Ting Ting Lin,[a] Hui Zhou[a] and Jianwei Xu[a,c*]

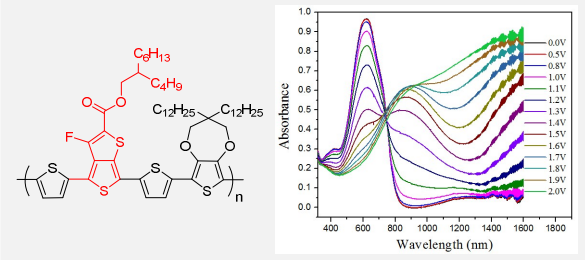

3-Fluorothieno[3,4-b]thiophene-2-carboxylate-based conjugated polymers were synthesized and their electrochromic devices displayed good optical contrasts, good coloration efficiencies and reasonable redox stability.